



# Mechanistic insight into cyclodextrin solubilization in aquoline: thermodynamics, structure, and molecular interactions

Emanuela Mangiacapre<sup>a</sup>, Alessandro Triolo<sup>b,\*</sup>, Miriana Kfoury<sup>c</sup>, Fabrizio Lo Celso<sup>d</sup>,  
Sophie Fourmentin<sup>c</sup>, Olga Russina<sup>a,\*</sup>

<sup>a</sup> Department of Chemistry, University of Rome Sapienza, Rome 00185, Italy

<sup>b</sup> Laboratorio Liquidi Ionici, Istituto Struttura della Materia, Consiglio Nazionale delle Ricerche (CNR-ISM), Rome 00133, Italy

<sup>c</sup> Univ. Littoral Côte d'Opale, UR 4492, UCEIV, Unité de Chimie Environnementale et Interactions sur le Vivant, F-59140 Dunkerque, France

<sup>d</sup> Department of Physics and Chemistry, University of Palermo, Palermo, Italy

## ARTICLE INFO

### Keywords:

Deep eutectic solvents  
Supramolecular organization  
Aggregation  
Hydrogen bonding  
Water in salt

## ABSTRACT

The development of new green solvent systems capable of enhancing cyclodextrin (CD) solubility is of primary importance in CD research. This need is particularly relevant for overcoming the poor aqueous solubility of native CDs, notably  $\beta$ -CD, while preserving their host-guest encapsulation ability. In this framework, several approaches have been investigated, including the use of Deep Eutectic Solvents (DESS)—a new class of promising green media—as well as compounds exhibiting hydrotropic behaviour. This work presents a comprehensive investigation into the solubility behaviour of the three native CDs ( $\alpha$ -,  $\beta$ -, and  $\gamma$ -CD) in different aqueous choline chloride (ChCl) mixtures at various water:ChCl molar ratios ( $n = 2, 3, 4, 6$  and  $10$ ). At  $n = 4$ , corresponding to a deep eutectic mixture (aquoline) Mangiacapre et al. (2023) [1], all CDs exhibit a maximum in solubility, exceeding in all cases values obtained from pure water. Thermodynamic analysis reveals that, in all the cases explored, the solubilization mechanism is endothermic; therefore, solubility increases with increasing temperature. Small-Angle X-ray Scattering (SAXS) experiments confirm the absence of CDs aggregation, even at concentrations approaching the solubility limits. Molecular Dynamics (MD) simulations provide insights into the solvation mechanism of  $\beta$ -CD in the mixture with  $n = 4$ , highlighting a cooperative network of hydrogen bonding, electrostatic, and dispersive interactions between the CD and the surrounding solvent species, with ions ( $\text{Cl}^- + \text{Ch}$ ) and water being comparably distributed around the  $\beta$ -CD. These findings indicate that aquoline provides a favourable solvation environment that enhances  $\beta$ -CD solubility while preventing flocculation, with ChCl likely exerting a hydrotropic effect.

## 1. Introduction

Cyclodextrins (CDs) are a family of naturally occurring cyclic oligosaccharides produced through the enzymatic degradation of starch by the bacterial enzyme cyclodextrin glucosyltransferase (CGTase). Structurally, natural CDs are composed exclusively of  $\alpha$ -1,4-linked D-glucopyranose units, and are classified according to the number of these units into three main types:  $\alpha$ -,  $\beta$ -, and  $\gamma$ -CD, consisting of six, seven, and eight D-glucopyranose monomers, respectively [2]. These are the primary cyclodextrins produced by the enzyme and are therefore referred to as 'native' CDs. From a structural point of view, CDs are cyclic oligosaccharides and belong to the broader class of cage molecules; they are characterized by a rigid, three-dimensional toroidal structure with a

hydrophobic internal cavity and a hydrophilic outer surface. This architecture enables CDs to form host-guest inclusion complexes with a wide variety of lipophilic compounds, making them highly versatile molecular containers [2–5]. Owing to these unique properties, CDs have found widespread applications across diverse sectors, including the food industry [6–10], cosmetics [9–11], pharmaceuticals, biomedicine [12–17], and in green and sustainable technologies [18–21]. However, industrial applications often demand formulations that are highly tailored and precisely optimized. In this context, the use of solvents that are both safe and easy to produce becomes crucial. Water is an appealing candidate due to its safety, availability, and environmental compatibility. On the other hand, native CDs display markedly different solubilities in water at room temperature: ca. 130 mg/ml for  $\alpha$ -CD, 18.5 mg/

\* Corresponding authors.

E-mail addresses: [triolo@ism.cnr.it](mailto:triolo@ism.cnr.it) (A. Triolo), [olga.russina@uniroma1.it](mailto:olga.russina@uniroma1.it) (O. Russina).

<https://doi.org/10.1016/j.molliq.2025.129117>

Received 15 November 2025; Accepted 7 December 2025

Available online 12 December 2025

0167-7322/© 2025 The Author(s). Published by Elsevier B.V. This is an open access article under the CC BY license (<http://creativecommons.org/licenses/by/4.0/>).

ml for  $\beta$ -CD, and 249 mg/ml for  $\gamma$ -CD [22,23], respectively. Among these,  $\beta$ -CD exhibits the lowest aqueous solubility, yet it remains the most attractive form, from an applicative standpoint, due to the size of its internal cavity, well-suited for a broad range of guest molecules, and its cost-effectiveness [24]. The low solubility of  $\beta$ -CD in aqueous environments is primarily attributed to the formation of strong hydrogen bonds between secondary hydroxyl groups of adjacent glucose units. These interactions restrict hydration on the secondary rim and increase the rigidity of the macrocycle, resulting in poor solvation [23,25,26]. Furthermore, native CDs are prone to forming large, poorly soluble aggregates in water, which further limits their effective uses in solution [27–30]. To address these limitations, several strategies have been investigated to improve the solubility of cyclodextrins, particularly the  $\beta$ -CD, in aqueous environments and to prevent their tendency to self-aggregate [31]. Among these approaches, the use of compounds with hydrotropic effect has emerged as particularly promising. Hydrotropes are compounds that enhance the solubility of poorly soluble substances in water by establishing more favourable interactions with the solute than those typically occurring between the solute and water [32].

One well-known example is urea, a small and highly water-soluble organic molecule, which has been shown to markedly increase the solubility of  $\beta$ -CD in aqueous media [33–35]. Recent studies have demonstrated that favourable interactions between urea and  $\beta$ -CD displace thermodynamically unfavourable water molecules from the  $\beta$ -CD surface and cavity, effectively reducing the free energy barrier for solvation [34,35]. In parallel, the exploration of unconventional solvents such as Deep Eutectic Solvents (DESs) has opened new avenues for CD solubilization. DESs are a class of sustainable and environmentally friendly media, typically composed of two or more components that form eutectic mixtures with melting points significantly lower than those of the individual constituents [36]. One of the most studied DESs is reline, a 1:2 mixture of choline chloride (ChCl) and urea [37]. Reline has been reported to dramatically enhance the solubility of  $\alpha$ -,  $\beta$ -, and  $\gamma$ -CD by factors of 3.5, 55, and 4, respectively, when compared to water [38]. A combination of Small-Angle X-ray Scattering (SAXS) and Molecular Dynamics (MD) simulations has provided insights into the mechanism underlying this solubility enhancement. The chloride anion forms strong hydrogen bonds with the hydroxyl groups of  $\beta$ -CD, while urea interacts with the hydrophobic regions of the macrocycle, reducing aggregation through dispersive interactions. These synergistic interactions between urea and choline chloride components are essential for the improved stability and solubility of  $\beta$ -CD in reline DES [39].

Interestingly,  $\beta$ -CD has been reported to exhibit limited solubility in other ChCl-based DESs, such as ethaline (ChCl:ethylene glycol, 1:2) and glyceline (ChCl:glycerol, 1:2) [39]. Moreover, it has been shown that the addition of water to reline (ChCl:urea, 1:2) can reduce the solubility of  $\beta$ -CD [34], and that the 1:2 ratio traditionally used to define reline does not correspond to the optimal condition for CD solubilization; in fact, it appears to be among the least effective [40]. These findings suggest that the solubility of CDs in DESs is generally governed by multiple, interdependent factors, including the specific components, their molar ratios, and the hydration level.

In this context, the solubility of the three native cyclodextrins, i-CDs (with  $i = \alpha, \beta, \text{ and } \gamma$ ), was investigated in a series of ChCl-water mixtures with varying water:ChCl molar ratios ( $n = 2, 3, 4, 6, \text{ and } 10$ ). Previous studies have shown that the ChCl/water system exhibits a deep eutectic character [1,41], with the mixture at  $n = 4$  (*aquoline*) corresponding to the true deep eutectic composition [1].

Solubility measurements were performed at three temperatures (293, 303, and 313 K) by means of polarimetric measurements. An in-depth thermodynamic analysis was then carried out to elucidate the nature of the solvation processes. SAXS experiments were subsequently performed to confirm the absence of CD aggregation in all ChCl-water mixtures, both near saturation and at lower concentrations. Finally, MD simulations were conducted to provide atomistic insight into the dissolution mechanism of  $\beta$ -CD within the deep eutectic ChCl-water

mixture at  $n = 4$  (*aquoline*). The combined use of experimental scattering techniques and MD simulations has proven to be a powerful and complementary approach for obtaining structural insight into CD solvation phenomena in media such as DESs [39,42,43].

In the broader context of cyclodextrin chemistry, this study contributes a new perspective on the role of solvent design and component synergy in optimizing solubility, a key parameter for many different CDs' applications.

## 2. Materials and method

### 2.1. Samples and mixtures' preparation

Choline Chloride (ChCl) was purchased from TCI Chemicals with a purity of 99.5 %.  $\alpha$ -Cyclodextrin,  $\beta$ -Cyclodextrin, and  $\gamma$ -Cyclodextrin ( $\alpha$ -CD,  $\beta$ -CD, and  $\gamma$ -CD, respectively) were supplied by Wacker-Chemie (Lyon, France). Before preparing the ChCl-water mixtures, ChCl was dried under high vacuum at approximately 353 K for 96 h to eliminate residual moisture, then stored in an anhydrous environment. The dried ChCl was precisely weighed, and Milli-Q water was added to obtain ChCl-water mixtures with varying molar ratios. Specifically, five different mixtures were prepared with water:ChCl molar ratios of  $n = 2, 3, 4, 6, \text{ and } 10$ . Each mixture was maintained at approximately 325 K under constant stirring until a clear and homogeneous liquid was obtained.

### 2.2. Karl-Fischer measurements

Before use, the exact water content in each ChCl-water mixture was determined using the Karl Fischer titration method with a DL31 Volumetric KF Titrator (Mettler Toledo DL31). Each measurement was performed at least three times to obtain an appropriate mean value with the associated deviation standard. Results in Table S1 of the ESI show that the measured molar ratios  $n$  completely matches the expected ones, demonstrating that all samples were accurately prepared.

### 2.3. Solubility analysis

The solubility analysis was performed adding an excess amount of i-CD ( $i = \alpha, \beta \text{ or } \gamma$ ) to each ChCl-water mixture. The solutions were then stirred and heated at selected temperatures (293 K, 303 K, and 313 K) for 24 h. Afterward, the solutions were centrifuged, and the supernatant was filtered through a 1.0  $\mu\text{m}$  J.T. Barker syringe filter with glass fibres and a 25 mm diameter. Accurate distilled water dilutions were subsequently prepared, and the optical rotation of each i-CD solution was measured using a Jasco P-2000 polarimeter. The concentration of dissolved CDs was then calculated from three standard curves corresponding to aqueous solutions of known concentrations of each i-CD (Fig. S1 of the ESI).

### 2.4. SAXS measurements

Small Angle X-ray Scattering (SAXS) experiments were carried out at the SAXS Lab Sapienza using a Xeuss 2.0 Q-Xoom system (Xenocs SA, Sassenage, France), equipped with a micro-focus Genix 3D X-ray source ( $\lambda = 0.1542 \text{ nm}$ ) and a two-dimensional Pilatus3 R 300 K detector. The measurements covered a Q range from 0.04  $\text{\AA}^{-1}$  to 0.6  $\text{\AA}^{-1}$ . Samples were prepared in ChCl-water mixtures at different molar ratios,  $n$ , each containing one of the i-CD ( $i = \alpha, \beta, \gamma$ ), with the CD concentration chosen based on solubility results. The solutions were loaded into 1 mm borosilicate capillaries, which were carefully sealed with hot glue to prevent evaporation. All measurements were conducted at room temperature (293 K).

#### 2.4.1. Analysis of SAXS data

SAXS patterns were analysed and fitted using the SASView software

(M. Doucet et al., SasView Version 6.0.1, <https://doi.org/10.5281/zenodo.1412041>), following the same approach adopted in previous studies [39,44]. Initially, each pattern was corrected for both solvent and background contributions. The corrected data were then modelled using the core-shell sphere model, which effectively represents isolated and isotropically oriented i-CDs.

For each dataset, the scaling factor, a residual background and the electron density (ED) of the shell were considered as fitting parameters. The i-CD structural dimensions (radius and shell thickness), the solvent and the core EDs were kept constant throughout the fitting process, after preliminary data analysis and also on the basis of our previous modelling of related systems. The choice of fixed structural parameters was based on our previous works [39,44], while the core ED was assumed to match the solvent ED and was calculated using the following equation:

$$\rho = \frac{\sum_i^n Z_i}{\bar{V}} \cdot r_e \quad (1)$$

Here,  $\rho$  represents ED,  $Z_i$  is the atomic number of atom  $i$  in the considered medium,  $r_e$  ( $2.81 \times 10^{-13}$  cm) represents the classical electron radius and  $\bar{V}$  is the molecular volume containing all  $n$  atoms.

Table S3 and Table S4 in the ESI summarize all constant values used in the fitting procedure. When required, hard sphere interactions were considered and modelled using the Percus-Yevick approximation [45,46], with an effective hard sphere radius equal to the outer radius of the i-CD and the volume fraction of the hard spheres.

## 2.5. Computational details

Molecular Dynamics (MD) simulations were performed using the GROMACS 2021.3 package [47,48]. Bonded and non-bonded parameters for  $\beta$ -CD were derived from q4-MD force field [49–51], while for choline chloride were described using an all-atoms OPLS force field developed by the group of Acevedo [52]; TIP3P potential was used for water [53].

The simulation for the probed mixture (aquoline,  $n = 4$ ) was performed using a cubic box; details concerning the number of species are shown in Table 1.

Periodic boundary conditions were applied. Initial configurations were created by Packmol software [54], the starting box dimension in the simulation was fixed at 7.5 nm. The equilibration procedure was done in several steps, starting from a NVT simulation at 400 K, followed by a series of NPT runs lowering progressively the temperature to their final value at 298 K, pressure was fixed for all system at 1 bar and a total of 8 ns equilibration runs were performed. After the equilibration phase, the system was run for a total of 50 ns for a production run at 298 K; then a final 2 ns trajectory was generated, and it was saved at a frequency of 1 ps for calculation of the structural properties. The simulation was always checked versus the density and energy profile. During the production runs for the temperature coupling, we used a velocity rescaling thermostat [55] (with a time coupling constant of 0.1 ps), while for the pressure coupling, we used a Parrinello–Rahman barostat [56] (1 ps for the relaxation constant). The Leap-Frog algorithm with a 1 fs time step was used for integrating the equations of motion. Cut-offs for the Lennard-Jones and real space part of the Coulombic interactions were set to 16 Å for all the systems. For the electrostatic interactions, the Particle Mesh Ewald (PME) summation method [57,58] was used, with an interpolation order of 6 and 0.08 nm of FFT grid spacing. Selected pair correlation function and angular distribution function were obtained by

**Table 1**

Details concerning the number of species employed to perform classical MD simulation.

N° of ChCl	N° of water	N° of $\beta$ -CD	ChCl:water: $\beta$ -CD	$\beta$ -CD (mg/ml)
1000	4200	20	1:4.2:0.02	116

TRAVIS [59–61].

## 3. Results and discussion

### 3.1. Solubility measurements

Polarimetry was used to determine the solubility of the three i-CDs (with  $i = \alpha, \beta$  and  $\gamma$ ) in all the ChCl-water systems as well as in pure water at three different temperatures (293 K, 303 K, and 313 K). Fig. 1 presents the solubility results for all the i-CDs, expressed in molarity (M), at specific temperatures as a function of the water content. Each measurement was repeated at least twice, and the error bars represent the standard error of the mean obtained from the replications.

From Fig. 1 clearly emerges the overall good agreement with the data reported by Jozwiakowski et al. on CDs solubility in pure water [22]. Moreover, the trend observed in Fig. 1 exhibits for all i-CDs a maximum around a water content of 35 wt%, corresponding to an  $n$  of approximately 4. In recent works this composition was evaluated as the one exhibiting deep eutectic nature, subsequently named as *aquoline* [1,41]. In all cases, the i-CDs' solubility increases compared to the case of pure water when water content reaches the composition of aquoline.

This trend may be attributed to the hydrotropic effect of ChCl, rarely discussed in the literature. Few studies have highlighted the potential hydrotropic effect of ChCl-based mixtures in enhancing the solubility of poorly water-soluble hydrophobic compounds [62]. The possible role of ChCl as a hydrotrope outside of eutectic mixture formulation has been explored in the field of surfactant systems: one study reported that the addition of ChCl to aqueous solutions of DABCO-16, a cationic surfactant, significantly enhanced the micellar solubilization of hydrophobic compounds such as Sudan I and curcumin [63]. Interestingly, ChCl has been shown to act as an effective hydrotrope also for Kraft lignin, markedly increasing its solubility in aqueous solutions. The maximum solubilization was observed at ChCl molar fractions between 0.20 and 0.25 (corresponding to molar ratios  $n = 4$  and  $n = 3$ , respectively) [64]. In the work of Cláudio et al., the role of ChCl as a hydrotrope was investigated for vanillin solubilization: a maximum in solubility was observed at approximately 20 wt% ChCl (corresponding to  $n \approx 30$ ) [65]. A similar trend was reported for ibuprofen, where the solubility peak occurred at around 40 wt% ChCl ( $n \approx 12$ ) [66]. However, in both cases, no broad concentration ranges of ChCl were examined, and no information regarding the drying procedure of ChCl was provided. Based on our results, this suggests that a more comprehensive exploration of ChCl concentrations is essential to fully understand its potential hydrotropic behaviour.

Although the solubility of various species typically reaches a plateau in the presence of a hydrotrope, ionic hydrotropes like ChCl can instead lead to a maximum in solubility, as observed in Fig. 1. This behaviour has been attributed to variations in the ratio of dissociated to associated ions in ionic hydrotropes, as well as changes in hydrotrope concentration and, consequently, in the effective volume of hydrotrope participating in solute solubilization [65,67].

Table 2 offers a clearer visualization of the solubility enhancement of i-CDs, presenting the specific solubility values (expressed in mg/ml) for each i-CD in aquoline at 298 K. These values were obtained from the Van't Hoff plots, described in the following section.

Table 2 highlights the solubility enhancement of all investigated i-CDs compared to the case of pure water. Although the solubility value obtained for  $\beta$ -CD is five times lower than what McCune et al. reported for reline ( $\approx 1000$  mg/ml) [38], it is noteworthy that a water-based solvent exhibits a significant solubility enhancement for all the probed cyclodextrins. This is particularly remarkable given the typical CDs' low solubility in aqueous solutions. Moreover, in the case of  $\beta$ -CD, a significant solubility enhancement compared to other DESs like ethaline (1:2 ChCl:ethylene glycol) or glyceline (1:2 ChCl:glycerol) is observed, where  $\beta$ -CD solubilizes only up to tens of milligrams at 293 K [39]. It is also important to highlight differences with the findings reported by

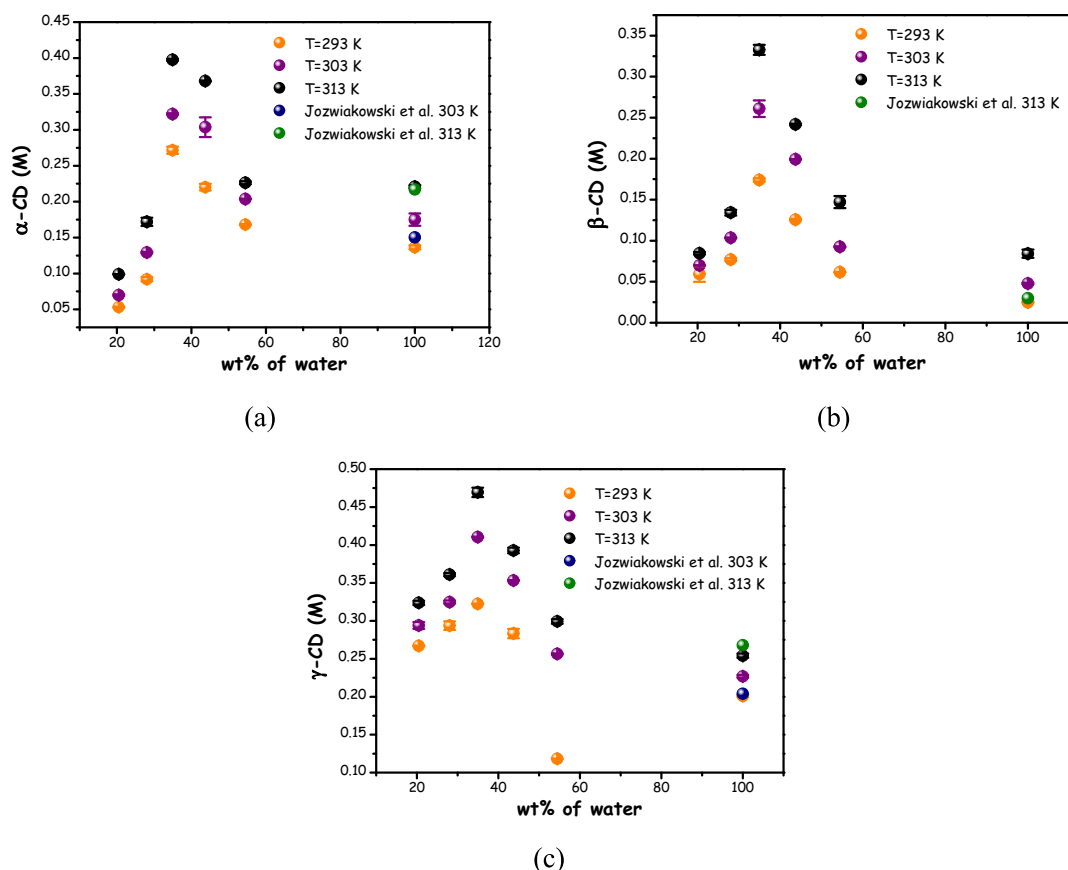


**Fig. 1.**  $\alpha$ -CD (a),  $\beta$ -CD (b) and  $\gamma$ -CD (c) solubility as function of water percentage (wt%) for all the explored ChCl-water mixtures at three different fixed temperatures: 293 K, 303 K and 313 K. For pure water, results are compared with those reported by Jozwiakowski et al. at 303 K and 313 K [22].

**Table 2**

Solubility values of i-CDs in aquoline compared to the solubility in pure water at 298 K, along with the corresponding enhancement factor. <sup>a</sup> [22]

i-CD	Solubility in aquoline (mg/ml)	Solubility in water (mg/ml)	Enhancement factor
$\alpha$	286	129.5 <sup>a</sup>	$\approx 2$
$\beta$	237	18.41 <sup>a</sup>	$\approx 13$
$\gamma$	467	249.2 <sup>a</sup>	$\approx 1.9$

Shumilin et al., who similarly to this work investigated the solubility of  $\beta$ -CD in ChCl aqueous solutions. However, when comparing mixtures with similar water content, their reported  $\beta$ -CD solubility values are generally lower than those obtained in this work. Moreover, in their case, the maximum solubility was reached at a water content of approximately 60 wt%, corresponding to a molar ratio of about  $n = 11$ , which contrasts with maximum observed here at  $n = 4$  [34] (Fig. S2 in the ESI).

### 3.2. Thermodynamic study

The natural logarithm of the mole fraction ( $x$ ) of the explored i-CDs, corresponding to their solubility in either the ChCl-water mixtures or pure water, is plotted as a function of temperature to construct the Van't Hoff plots (Fig. 2). These data are used to calculate the Gibbs free energy of solution ( $\Delta G_{s,0}$ ), the enthalpy of solution ( $\Delta H_{s,0}$ ), and the entropy of solution ( $\Delta S_{s,0}$ ) at each temperature using the following equations:

$$\Delta G_{\text{sol}} = -RT \ln(x) \quad (2)$$

$$\Delta H_{\text{sol}} = RT^2 \frac{d \ln(x)}{dT} \quad (3)$$

$$\Delta S_{\text{sol}} = \Delta H_{\text{sol}} - \Delta G_{\text{sol}} \quad (4)$$

As an example, Table 3 presents all the results for  $\beta$ -CD, while the parameters obtained for  $\alpha$ -CD and  $\gamma$ -CD are provided in the ESI (Tables S5 and S6, respectively).

Notably, for all the explored i-CDs, a  $\Delta G_{s,0} > 0$  is found, indicating that solvation is not a thermodynamically spontaneous process. Moreover, the process results to be endothermic with  $\Delta H_{s,0} > 0$ , meaning solubility increases as temperature rises. This is consistent with literature data reporting positive dissolution enthalpies for  $\beta$ -cyclodextrin in aqueous media, including systems containing 6 % sucrose, 8 % NaCl, and their mixture, obtained through van't Hoff analysis [68].

It is also noteworthy that  $T \cdot \Delta S_{s,0}$  is generally positive, suggesting an increase in disorder upon solvation. However, some exceptions arise:  $\alpha$ -CD in the ChCl-water mixture with  $n = 10$  at all temperatures,  $\beta$ -CD in the mixture at  $n = 2$  at 293 K, and  $\gamma$ -CD in the system with  $n = 2$  across all examined temperatures. This result is generally attributed to an overall increase of the order within the system. Indeed, there are systems where a loss of entropy upon dissolution has been observed: the case of alkali metal halides dissolved in ionic liquids [69], hydrophobic solutes in water [70], or highly charged ions in aqueous solutions [71]. A single, unified explanation for this behaviour remains elusive, as entropy loss can manifest in various ways. These include restrictions in molecular dynamics, such as reduced mobility within hydrogen-bond networks, indicating that the solvent has become more structured [69]. Furthermore, in all cases enthalpy plays a dominant role in the solvation process: for each system,  $\Delta H_{s,0} > T \cdot \Delta S_{s,0}$  is observed, indicating that solvation is primarily driven by enthalpic contributions. This suggests

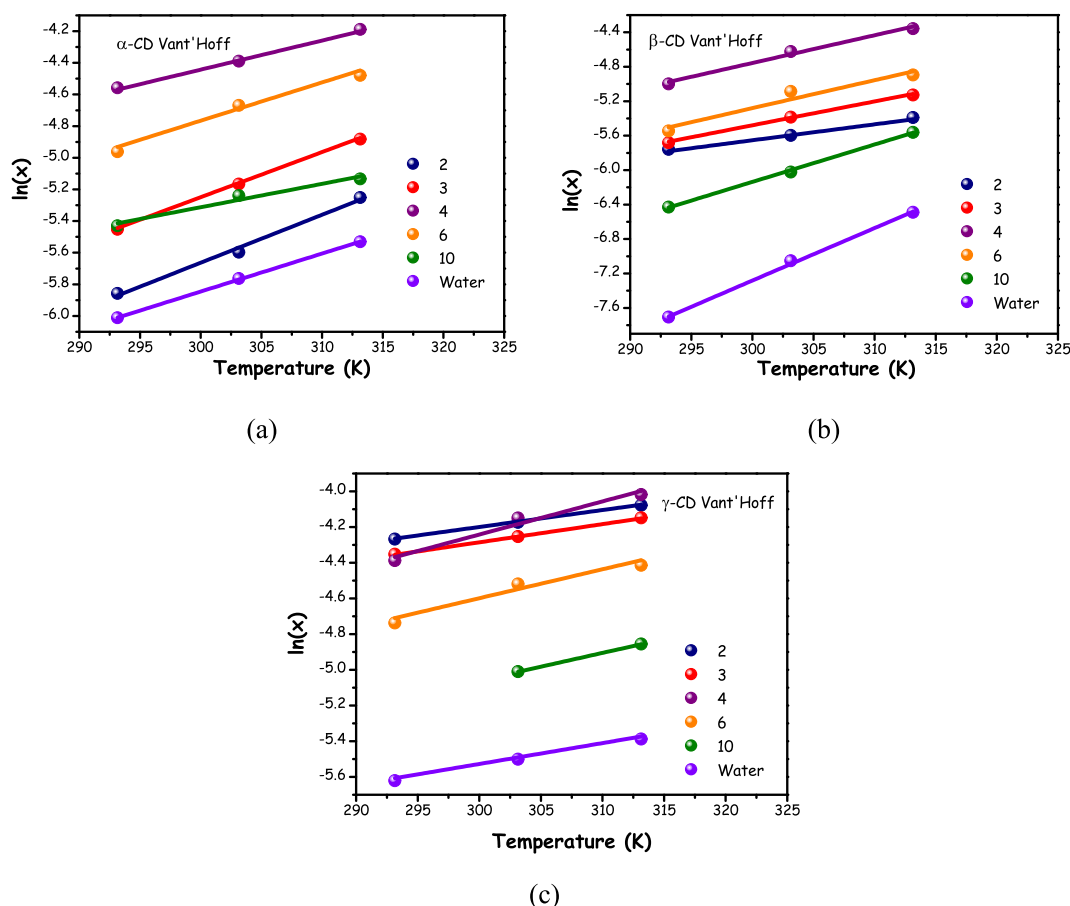


**Fig. 2.** Van't Hoff plots for  $\alpha$ -CD (a),  $\beta$ -CD (b) and  $\gamma$ -CD (c) in all the explored ChCl-water mixtures. Solid lines represent the linear fit employed to obtain the thermodynamic parameters.

**Table 3**

Solution thermodynamic parameters obtained at 293 K, 303 K and 313 K for  $\beta$ -CD dissolved in the explored ChCl-water mixtures.

$\Delta G_{\text{sol}}$ (kJ/mol) for $\beta$ -CD						
T (K)	ChCl:W n = 2	ChCl:W n = 3	ChCl:W n = 4	ChCl:W n = 6	ChCl:W n = 10	Water
293	14.04	13.85	12.18	13.52	15.67	18.79
303	14.11	13.58	11.65	12.82	15.18	17.78
313	14.03	13.35	11.34	12.75	14.48	16.90
$\Delta H_{\text{sol}}$ (kJ/mol) for $\beta$ -CD						
T (K)	ChCl:W n = 2	ChCl:W n = 3	ChCl:W n = 4	ChCl:W n = 6	ChCl:W n = 10	Water
293	13.22	19.79	22.94	23.22	31.01	43.51
303	14.14	21.17	24.53	24.83	33.16	46.53
313	15.08	22.58	26.17	26.50	35.39	49.65
$T \cdot \Delta S_{\text{sol}}$ (kJ/mol) for $\beta$ -CD						
T (K)	ChCl:W n = 2	ChCl:W n = 3	ChCl:W n = 4	ChCl:W n = 6	ChCl:W n = 10	Water
293	-0.820	5.942	10.75	9.706	15.34	24.73
303	0.025	7.590	12.87	12.01	17.98	28.75
313	1.053	9.231	14.83	13.75	20.90	32.76

that stronger interactions occur between the solvent components rather than between the solvent and solute. These results are similar to those obtained for the solubilization of  $\beta$ -CD in hydrophilic ionic liquids [72], as well as for  $\alpha$ -CD in the 1-ethyl-3-methylimidazolium acetate ionic liquid [44]. On the other hand, results presented in this work contrast with the findings for  $\beta$ -CD dissolution in reline, where dissolution calorimetry measurements indicate an exothermic dissolution process [73].

### 3.3. SAXS measurements

The aggregation of CDs in aqueous solutions is a well-documented phenomenon. Numerous studies have reported their natural tendency

to form aggregates in pure water [74–76], even at dilute concentrations below their solubility limits [27,77]. Despite these observations, SAXS and SANS measurements performed on both  $\beta$ -CD and  $\gamma$ -CD in aqueous solutions at dilute regimes do not indicate the presence of any aggregation [78]; the same conclusion is supported by various NMR studies conducted in aqueous solutions of  $\alpha$ -CD,  $\beta$ -CD, and  $\gamma$ -CD [79,80]. Considering this, SAXS measurements on a series of i-CDs solutions in ChCl–water mixtures were conducted. Following recent studies on  $\beta$ -CD solvation in reline [39] and the solubilization of  $\alpha$ -CD,  $\beta$ -CD, and  $\gamma$ -CD in the ionic liquid 1-ethyl-3-methylimidazolium acetate (IL) [44], the scattering patterns were analysed using a model based on identical spherical shells. These shells represent the structure of monomeric  $\alpha$ -CD,  $\beta$ -CD, and  $\gamma$ -CD, whose mutual interactions can be described by a hard

sphere potential. Therefore, each scattering pattern was modelled using the following mathematical approach:

$$I(Q) = A \bullet P(Q) \bullet S(Q) + \text{bkg} \quad (5)$$

where  $A$  is a scaling factor,  $\text{bkg}$  represents a constant background level, and  $P(Q)$  and  $S(Q)$  correspond to the form factor and structure factor, respectively [39,44]. By applying the previously described model and performing the pattern analysis detailed in Section 2.4.1, fits presented in Figs. S3, S4 and S5 of the ESI were obtained. Specifically, experiments were performed on solutions obtained by dissolving  $\beta$ -CDs in selected ChCl-water mixtures, at concentrations close to the experimental maximum solubility obtained at 293 K.

In all the cases presented, the applied models accurately describe the SAXS patterns, leading to the conclusion that CDs' aggregation is absent across all the explored conditions. Notably, in each mixture, the CD concentration was chosen close to its maximum solubility at 293 K. Although in some instances the  $\beta$ -CDs solubility was lower than that observed in pure water, the absence of aggregation is crucial for potential CDs' applications. Aggregation or flocculation of CDs can significantly impact their encapsulation capabilities, thereby reducing their effectiveness in drug solubilization and delivery [28,81,82].

Considering solubility results and the particular importance of  $\beta$ -CD, SAXS patterns for various  $\beta$ -CD solutions in aquoline at different CD content were analysed (Fig. 3).

The excellent agreement between SAXS data and the employed model, in all the probed cases, confirms the absence of  $\beta$ -CD aggregation in aquoline. This strongly suggests that the solvent effectively stabilizes  $\beta$ -CD as individual molecules, even at the highest tested concentrations.

### 3.4. Molecular Dynamics (MD) simulation results

Molecular Dynamics (MD) simulation was performed on the  $\beta$ -CD/aquoline system. The aim was to identify the key interactions driving the  $\beta$ -CD solvation in the best ChCl-water mixture in terms of solubility enhancement.

Fig. 4 displays the nomenclature used in the MD analysis for each atom of every species involved in the studied system.

Specifically, the MD analysis was conducted on a  $\beta$ -CD/aquoline solution in which the concentration of  $\beta$ -CD corresponds to approximately half of its maximum solubility at 298 K. This condition translates into a ChCl:water: $\beta$ -CD molar ratio of 1:4.2:0.02 (see Table 1 for details).

The structural correlations between  $\beta$ -CD and the solvating components of aquoline were analysed using Radial Distribution Functions (RDFs), which show the normalized densities of choline (Ch), chloride ( $\text{Cl}^-$ ), and water centre of masses (CoM) with respect to the CoM of a

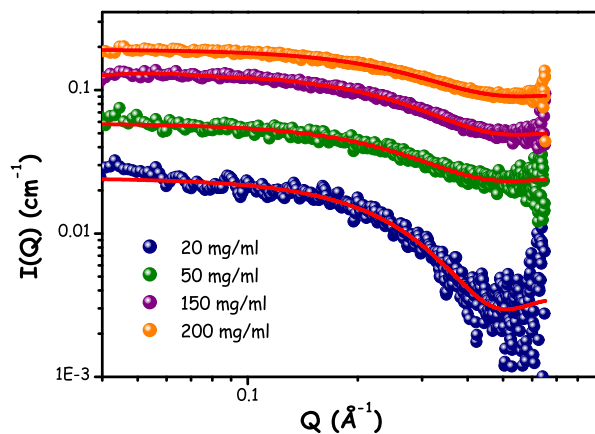


Fig. 3. SAXS patterns of  $\beta$ -CD in Aquoline at varying concentrations, recorded at room temperature. The continuous lines represent fits based on isolated  $\beta$ -CD molecules dissolved in the mixture.

reference  $\beta$ -CD (Fig. 5). The light grey shaded area represents the  $\beta$ -CD wall, determined by calculating the intramolecular RDF between the  $\beta$ -CD CoM and all its constituent atoms. The RDF of water oxygen atom around  $\beta$ -CD in pure water is also shown for sake of comparison.

From Fig. 5 it clearly emerges that all aquoline components can reside within the cavity of the reference  $\beta$ -CD (i.e., for distances  $r \leq 4 \text{ \AA}$ ). The number of nearest neighbours for all the correlations presented in Fig. 5, obtained by integrating up to a distance of  $4.0 \text{ \AA}$ , are shown in Table S8 of the ESI. Table S8 reveals an interesting trend: unlike reline, where two urea molecules are consistently included within the  $\beta$ -CD cavity [39], aquoline exhibits a similar but lower inclusion of water molecules, despite their higher amount in the system. Comparing to reline, the number of  $\text{Cl}^-$  anions remain essentially unchanged (most likely being bound to the hydrophilic CD rims), while the number of choline molecules within the cavity is quite similar. In the case of pure water, the preferential inclusion of water molecules is observed, with approximately 9.0 water oxygen atoms located inside the cyclodextrin cavity.

An examination of the exterior region of  $\beta$ -CD reveals that all aquoline species form well-defined solvation shells in close proximity to its outer surface. Interestingly, a solvation distance sequence can be identified: the  $\beta$ -CD-water correlation exhibits a peak centred around  $9.2 \text{ \AA}$ , followed closely by the  $\beta$ -CD- $\text{Cl}^-$  correlation at approximately  $9.3 \text{ \AA}$ , and finally the choline solvation shell, with a peak centred at approximately  $10.3 \text{ \AA}$ . This behaviour differs from the case of reline, where the chloride ion approaches  $\beta$ -CD first, followed by urea [39]. Here, likely due to the small size of water molecule, water and chloride appear to concomitantly approach the  $\beta$ -CD wall. From previous studies [25,39,83], the RDF for pure water exhibits a weak peak in the outer region, centered around  $9.5 \text{ \AA}$ , with no evidence of a second solvation shell at longer distances. The number of nearest neighbours concerning the external solvation shells for all aquoline species is reported in Table S9 of the ESI. A comparison with reline case reveals a similar number of chloride anions surrounding the  $\beta$ -CD, but a higher presence of choline species [39].

Given the variety of chemical species in the system, each of them bearing functional groups capable of acting as either hydrogen bond donors or acceptors, a detailed investigation of hydrogen bonding interactions is essential. Fig. 6 illustrates all the correlations between the hydroxyl oxygens of  $\beta$ -CD and the hydroxyl hydrogens of both water and Ch in aquoline.

Fig. 6 (a) and (b) reveal that all the correlations related to Oa and Od species display relatively sharp peaks around  $2.0 \text{ \AA}$ , which are consistent with hydrogen bonding interactions. While correlations involving Ob oxygen atoms exhibit weak yet appreciable features in both water and choline patterns, those involving Oc species display poorly defined or absent peaks, indicating weak to negligible hydrogen bonding, respectively. Interestingly, all the correlations involving water present intensities below unity, but appear slightly more structured and sharper than those involving Hch.

Key differences among the correlations shown in Fig. 6 become evident upon examination of the corresponding number of nearest neighbours reported in Table 4.

Table 4 reveals that the  $\beta$ -CD oxygen atoms Oa and Od are the most effectively involved in hydrogen bonding with water and Ch, as indicated by the high coordinating numbers of both Hw and Hch. In contrast, ether oxygens Ob and Oc appear to play a negligible role in hydrogen bonding with either water or Ch. These findings differ from what was observed in the case of reline, where urea, acting as the HBD, was able to form strong HBs with all the hydroxyl oxygen atoms of  $\beta$ -CD. In that system, all oxygen atoms exhibited  $N(r)$  values equal to or greater than 0.25, indicating more effective interactions [39], fingerprinting a closer approach of urea to the hydrophobic portion of  $\beta$ -CD.

The hydrogen bonding interactions where water oxygen and chloride serve as HBA with the hydroxyl hydrogens of cyclodextrin are also explored (Fig. 7).

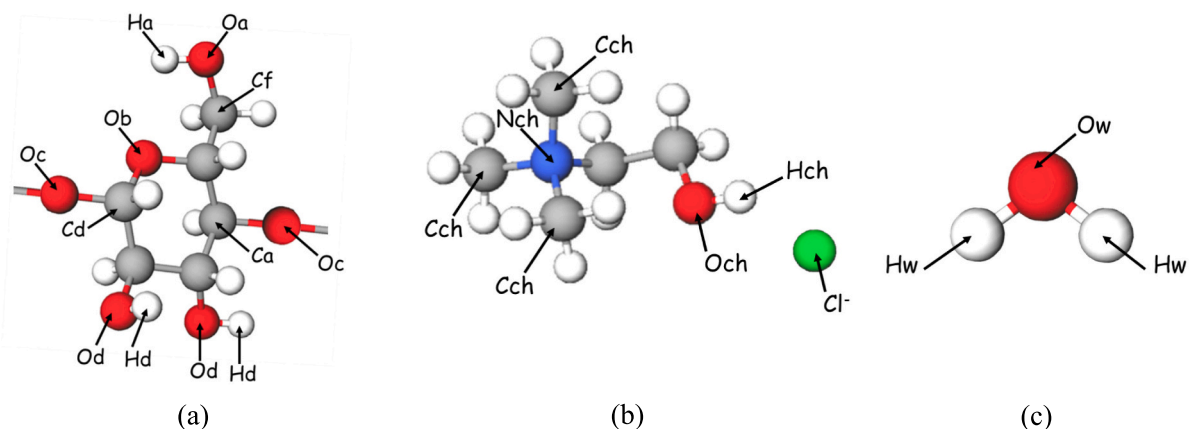


Fig. 4. Schematic representation of a  $\beta$ -CD monomer (a) on the left, choline and chloride (b) in the middle and water (c) on the right side.

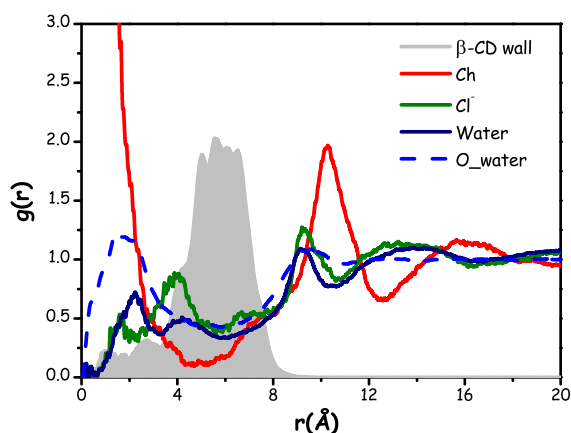


Fig. 5. Selected MD-computed RDFs between  $\beta$ -CD CoM and Ch (a), Cl<sup>-</sup> (b) and water (c) CoMs. The light grey shadowed area represents the  $\beta$ -CD wall. The dashed blue-line refers to the distribution of water oxygen atoms around the reference  $\beta$ -CD, taken from Ref. [39] for comparison purposes. (For interpretation of the references to colour in this figure legend, the reader is referred to the web version of this article.)

Therein, it emerges that both Cl<sup>-</sup> and Ow act as efficient hydrogen bond acceptors (HBAs), with strong interactions, as reflected by pronounced peaks at approximately 2.0 Å and 1.8 Å, respectively. These observations are consistent with previous findings for the reline system, where  $\beta$ -CD is strongly solvated via hydrogen bonds with both Cl<sup>-</sup> and the oxygen atom of urea. In reline, the urea oxygen shows a peak at a

greater distance than Cl<sup>-</sup> [39], whereas in aquoline the opposite trend is observed, with water exhibiting a closer correlation than chloride.

The effectiveness of all the HBs shown in Fig. 7 is also demonstrated by the number of nearest neighbours for both Cl<sup>-</sup> and Ow species around the hydroxyl hydrogens of  $\beta$ -CD (Table 5).

Data in Table 5 confirm the strong HBA character of Cl<sup>-</sup> toward the hydroxyl hydrogens of  $\beta$ -CD, with both Ha and Hd showing a relatively high number of coordinating chloride ions. These results also emphasize the key role of water: compared to reline, the number of coordinating Ow atoms far exceeds the number of Ou atoms from urea for both hydroxyl positions [39]. To provide a comprehensive overview of the hydrogen bonding interaction pattern, correlations between the choline oxygen atom (Och) and the hydroxyl hydrogens of  $\beta$ -CD were also analysed (Fig. S6 of the ESI). In both cases, the peaks are not well-defined and display two main features: a low-intensity peak centred

Table 4

Number of nearest oxygen neighbours  $N(r)$  related to the hydrogen bonding correlations between the hydroxyl oxygens of  $\beta$ -CD (Oa, Ob, Oc and Od) and the hydrogen atoms of water (Hw), urea (Hu) in reline [39] and choline (Hch).

N(r) at $r \leq 2.5$ Å					
Correlation	Aquoline	Correlation	Reline	Correlation	Aquoline
Oa-Hw	0.37	Oa-Hu	1.0 (2.9) <sup>b</sup>	Oa-Hch	0.10
Ob-Hw	0.17	Ob-Hu	0.46 (2.8) <sup>b</sup>	Ob-Hch	0.04
Oc-Hw	0.03	Oc-Hu	0.25 (3.0) <sup>b</sup>	Oc-Hch	0.01
Od-Hw	0.34	Od-Hu	0.77 (2.9) <sup>a,b</sup>	Od-Hch	0.06

<sup>a</sup> Average of the  $N(r)$  values for the two secondary hydroxyl hydrogens of  $\beta$ -CD from [39].

<sup>b</sup> Integration distance different from 2.5 Å, shown in the brackets.

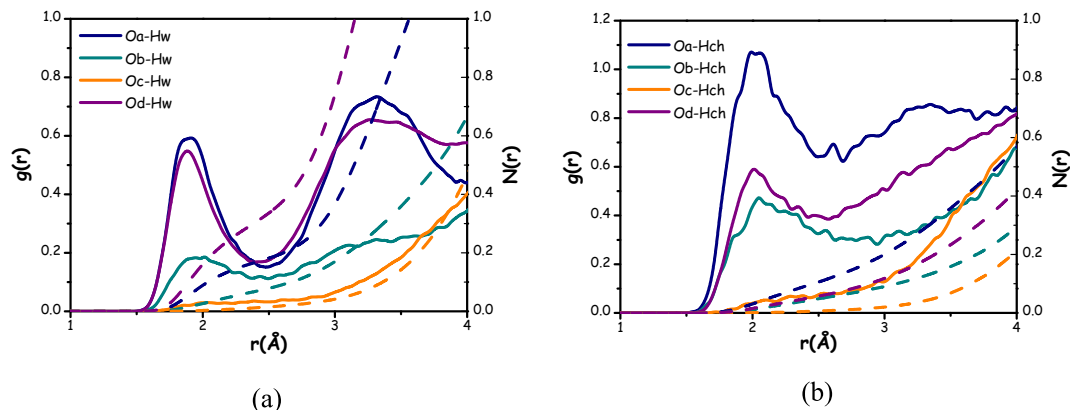


Fig. 6. RDFs (continuous lines) and corresponding running neighbour numbers (dashed lines) for all the Ox $\cdots$ Hw (a) and Ox $\cdots$ Hch (b) correlations (x = a, b, c and d).

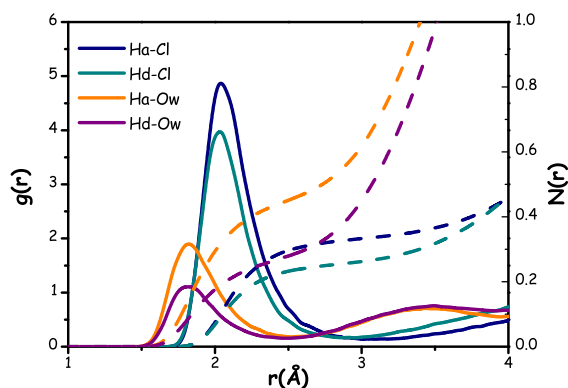


Fig. 7. RDFs (continuous lines) and corresponding running neighbour numbers (dashed lines) for the Hx...Cl<sup>-</sup> and Hx...Ow correlations (x = a and d).

Table 5

Number of nearest oxygen neighbours  $N(r)$  related to the hydrogen bonding correlations between the hydroxyl hydrogens of  $\beta$ -CD (Ha and Hd) and Cl<sup>-</sup> and the oxygen atom of water (Ow). For comparison, the coordination numbers of Cl<sup>-</sup> and Ou (urea oxygen) in reline were also reported [39].

N(r) at $r \leq 3.0 \text{ \AA}$			
Correlation	Aquoline	Correlation	Reline
Ha-Cl	0.33	Ha-Cl	0.70
Hd-Cl	0.26	Hd-Cl	0.51 <sup>a</sup>
Ha-Ow	0.63	Ha-Ou	0.22 (3.2 Å) <sup>b</sup>
Hd-Ow	0.46	Hd-Ou	0.06 (2.7 Å) <sup>a,b</sup>

<sup>a</sup> Average of the  $N(r)$  values for the two secondary hydroxyl hydrogens of  $\beta$ -CD from [39].

<sup>b</sup> Integration distance different from 3.0 Å, shown in the brackets.

around 2.0 Å, indicating relatively weak hydrogen bonding interactions between the species, and a broader signal that extends from approximately 3 Å to around 6 Å. These observations suggest that Ch behaves more effectively as hydrogen bond donor (HBD) rather than HBA, also considering results from Fig. 6.

Table S10 in the ESI presents the number of nearest neighbours associated with the correlations displayed in Fig. S6. As shown in Table S10, the number of Och species coordinating Ha and Hd is low, consistent with observations in the reline system [39], thus confirming the limited ability of choline to act as HBA toward the hydroxyl groups of  $\beta$ -CD.

The role of the ammonium moiety in choline is also examined. In particular, its positive charge may engage in electrostatic interactions with the hydroxyl groups of  $\beta$ -CD, while the surrounding methyl groups could contribute to dispersive interactions with the wall of the cyclodextrin. Relevant and selected correlations are presented in Fig. S7 of the ESI. Fig. S7 (a) demonstrates a strong affinity of the ammonium group for both Oa and Od species, as indicated by a relatively sharp peak centred around 4.3 Å, suggesting well-defined electrostatic interactions. Simultaneously, evidence of dispersive interactions is also observed: the presence of structured features in the 4–7 Å range for all the examined carbon sites along the  $\beta$ -CD wall is consistent with interactions between the outer surface of  $\beta$ -CD and the methyl groups surrounding the choline's ammonium moiety (Fig. S7 (b)). The most prominent peak is associated with the Cf site, which corresponds to the most solvent-exposed carbon atom on the  $\beta$ -CD surface. Its sharp and intense peak points to a preferential spatial correlation with the trimethylammonium group of choline, likely driven by dispersive forces. Drawing a parallel with reline, where a similar behaviour is observed due to the ammonium groups of urea [39], it can be suggested that, although less prominent than hydrogen bonding interactions, dispersive interactions may also play a role in preventing  $\beta$ -CD aggregation. Table S11 in the ESI

summarizes the number of nearest neighbours corresponding to the correlations presented in Fig. S7.

Overall, the MD analysis reveals a complex network of interactions involving all aquoline components in solvating  $\beta$ -CD. By considering the total number of nearest neighbours reported in Table S8 and Table S9 in the ESI, the resulting distribution of ions (Cl<sup>-</sup> and Ch) and water molecules, shown in Fig. 8, indicates a nearly 40:60 ratio, with water prevalence. This distribution, notably differing from aquoline bulk composition, likely underlies the observed solubility maximum at the specific aquoline molar ratio ( $n = 4$ ), highlighting the potential role of ChCl as a hydrotrope. Rather than being driven by the deep eutectic nature of aquoline, the solubility enhancement appears to stem from the ability of ChCl to organize around  $\beta$ -CD while simultaneously allowing an optimal amount of water to interact with it. At the aquoline composition, this balanced arrangement gives rise to a rich interplay of interactions, including hydrogen bonds mainly with hydroxyl groups of  $\beta$ -CD, as well as electrostatic and dispersive forces.

#### 4. Conclusions

This study presents a comprehensive solubility assessment of the three native cyclodextrins ( $\alpha$ -,  $\beta$ -, and  $\gamma$ -CD) in aqueous choline chloride (ChCl) mixtures across varying water:ChCl molar ratios ( $n = 2, 3, 4, 6$  and 10) and temperatures (293, 303, and 313 K). Polarimetric measurements show that all investigated CDs exhibit maximum solubility at  $n = 4$ , corresponding to the deep eutectic composition of the ChCl-water system (aquoline), where their solubility surpasses that in pure water.  $\beta$ -CD, the least water-soluble native CD, shows an increase in solubility of  $\sim 13$  times at this molar ratio compared to water. Thermodynamic analysis via Van't Hoff plots indicate that the solvation mechanism is in all cases endothermic ( $\Delta H_{s,d} > 0$ ), with solubility increasing with temperature. Small-Angle X-ray Scattering (SAXS) measurements confirm the absence of CDs' aggregation in all tested ChCl-water mixtures, even near saturation levels.

Classical Molecular Dynamics (MD) carried out on the  $\beta$ -CD/aquoline system provided atomistic detail to the characterization. Analysis of the solvation environment reveals that  $\beta$ -CD is surrounded by an approximately 40:60 ratio of ionic species (Cl<sup>-</sup> and Ch) and water molecules. This distribution suggests that the experimentally observed solubility maximum at  $n = 4$  likely arises from the cooperative contribution of both ions and water. Within this network, Cl<sup>-</sup> and water act as effective hydrogen-bond acceptors (HBAs), particularly toward the Ha and Hd hydroxyl hydrogens of  $\beta$ -CD. In contrast, choline primarily behaves as a hydrogen-bond donor (HBD) toward the Oa and Od oxygen atoms of  $\beta$ -CD, while also participating in electrostatic interactions through its ammonium group and dispersive contacts via its methyl groups with the outer surface of the macrocycle. At aquoline composition, this balanced interplay of interactions enhances  $\beta$ -CD solubility while preventing aggregation, suggesting a potential hydrotropic role of

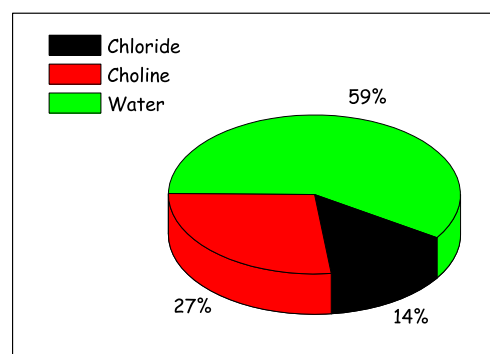


Fig. 8. Relative distribution of water, Cl and Ch ions involved in the first solvation shell of  $\beta$ -CD.

ChCl rather than attributing the solubility behaviour to aquoline deep eutectic nature.

Although aquoline offers a favourable solvation environment for  $\beta$ -CD, its effect is less pronounced than in reline. Systematic comparison with reline highlights the superior ability of urea, acting as a strong HBD in synergy with  $\text{Cl}^-$  (Table 4 and Table 5, respectively), to enhance  $\beta$ -CD solubility. This is consistent with previous observations where urea, upon addition to ChCl-water mixtures, promotes the exclusion of water from the immediate outer surface of  $\beta$ -CD [34]. However, the present study adds a new piece to the broader puzzle of CD research by demonstrating, through the combined use of experimental and computational approaches, that the solubility of native CDs can be significantly enhanced using water-based and environmentally friendly media. In particular, aquoline emerges as a promising, sustainable, and aggregation-free solvent platform for CDs applications.

#### Declaration of generative AI and AI-assisted technologies in the manuscript preparation process

During the preparation of this work the authors used ChatGPT in order to revise grammar, spelling and punctuation and apply minor rephrasing to text. After using this tool/service, the authors reviewed and edited the content as needed and take full responsibility for the content of the published article.

#### CRediT authorship contribution statement

**Emanuela Mangiacapre:** Conceptualization, Data curation, Formal analysis, Investigation, Methodology, Writing – original draft, Writing – review & editing. **Alessandro Triolo:** Conceptualization, Funding acquisition, Investigation, Methodology, Project administration, Supervision, Writing – review & editing. **Miriana Kfoury:** Data curation, Investigation, Methodology, Resources. **Fabrizio Lo Celso:** Data curation, Formal analysis, Investigation, Methodology, Software. **Sophie Fourmentin:** Conceptualization, Investigation, Methodology, Resources, Supervision, Validation, Writing – original draft. **Olga Russina:** Conceptualization, Data curation, Funding acquisition, Investigation, Methodology, Project administration, Supervision, Writing – review & editing.

#### Declaration of competing interest

The authors declare that they have no known competing financial interests or personal relationships that could have appeared to influence the work reported in this paper.

#### Acknowledgments

This work has been partially supported by the University of Rome Sapienza Projects: “Supra-DES in action” (AR123188A08DF1D1), “Chemical physical properties and solvation capability of water-based eutectic solvents” (RM123188F106B148) and “Hydrophilic vs hydrophobic eutectic solvents for oligosaccharides.” (RM12218152014836). Expert support from Dr. A. Del Giudice and access to the SAXS-Lab at the University of Rome Sapienza is acknowledged.

Research at ISM-CNR was partially supported by the project ECS00000024 “Ecosistemi dell’Innovazione”—Rome Technopole of the Italian Ministry of University and Research, public call n. 3277, PNRR—Mission 4, Component 2, Investment 1.5, financed by the European Union, Next Generation EU.

This work was also partially supported by PRIN2022 (“SEED4-GREEN”), sponsored by the European Union, Next Generation EU, Missione 4 Componente 1 (RG11715C7CC660BE).

#### Appendix A. Supplementary data

Supplementary data to this article can be found online at <https://doi.org/10.1016/j.molliq.2025.129117>.

#### Data availability

Data will be made available on request.

#### References

- [1] E. Mangiacapre, F. Castiglione, M. D’Aristotle, V. Di Lisio, A. Triolo, O. Russina, Choline chloride-water mixtures as new generation of green solvents: A comprehensive physico-chemical study, *J. Mol. Liq.* 383 (2023) 122120, <https://doi.org/10.1016/j.molliq.2023.122120>.
- [2] G. Crini, S. Fourmentin, É. Fenyvesi, G. Torri, M. Fourmentin, N. Morin-Crini, Fundamentals and Applications of Cyclodextrins, 2018, pp. 1–55, [https://doi.org/10.1007/978-3-319-76159-6\\_1](https://doi.org/10.1007/978-3-319-76159-6_1).
- [3] A. Cid-Samamed, J. Rakmai, J.C. Mejuto, J. Simal-Gandara, G. Astray, Cyclodextrins inclusion complex: preparation methods, analytical techniques and food industry applications, *Food Chem.* 384 (2022), <https://doi.org/10.1016/j.foodchem.2022.132467>.
- [4] J. Szejtli, Past, present, and future of cyclodextrin research\*, *Pure Appl. Chem.* 76 (10) (2004) 1825–1845, <https://doi.org/10.1351/pac200476101825>.
- [5] J. Szejtli, Introduction and general overview of Cyclodextrin chemistry, *Chem. Rev.* 98 (1998) 1743–1754, <https://doi.org/10.1021/cr970022c>.
- [6] J.M. López-Nicolás, P. Rodríguez-Bonilla, F. García-Carmona, Cyclodextrins and antioxidants, *Crit. Rev. Food Sci. Nutr.* 54 (2014) 251–276, <https://doi.org/10.1080/10408398.2011.582544>.
- [7] A.G. Pereira, M. Carpena, P.G. Oliveira, J.C. Mejuto, M.A. Prieto, J.S. Gandara, Main applications of cyclodextrins in the food industry as the compounds of choice to form host–guest complexes, *Int. J. Mol. Sci.* 22 (2021) 1–23, <https://doi.org/10.3390/ijms22031339>.
- [8] M. Fenyvesi, L. Vikmon, Szente, Cyclodextrins in food technology and human nutrition: benefits and limitations, *Crit. Rev. Food Sci. Nutr.* 56 (2016) 1981–2004, <https://doi.org/10.1080/10408398.2013.809513>.
- [9] S. Christaki, E. Spanidi, E. Panagiotidou, S. Athanasopoulou, A. Kyriakoudi, I. Mourtzinos, K. Gardikis, Cyclodextrins for the delivery of bioactive compounds from natural sources: medicinal, food and cosmetics applications, *Pharmaceuticals* 16 (2023), <https://doi.org/10.3390/ph16091274>.
- [10] G. Crini, É. Fenyvesi, L. Szente, Outstanding contribution of professor József Szejtli to cyclodextrin applications in foods, cosmetics, drugs, chromatography and biotechnology: a review, *Environ. Chem. Lett.* 19 (2021) 2619–2641, <https://doi.org/10.1007/s10311-020-01170-y>.
- [11] L. Ferreira, F. Mascarenhas-Melo, S. Rabaça, A. Mathur, A. Sharma, P.S. Giram, K. D. Pawar, A. Rahdar, F. Raza, F. Veiga, P.G. Mazzola, A.C. Paiva-Santos, Cyclodextrin-based dermatological formulations: Dermatopharmaceutical and cosmetic applications, *Colloids Surf. B: Biointerfaces* 221 (2023) 113012, <https://doi.org/10.1016/j.colsurfb.2022.113012>.
- [12] Y. Han, W. Liu, J. Huang, S. Qiu, H. Zhong, D. Liu, J. Liu, Cyclodextrin-based metal-organic frameworks (CD-MOFs) in pharmaceuticals and biomedicine, *Pharmaceutics* 10 (2018) 271, <https://doi.org/10.3390/pharmaceutics10040271>.
- [13] H.M.S.H. Soe, T. Loftsson, P. Jansook, The application of cyclodextrins in drug solubilization and stabilization of nanoparticles for drug delivery and biomedical applications, *Int. J. Pharm.* 666 (2024) 124787, <https://doi.org/10.1016/j.ijpharm.2024.124787>.
- [14] H. Shao, M. Liu, H. Jiang, Y. Zhang, Polysaccharide-based drug delivery targeted approach for colon cancer treatment: A comprehensive review, *Int. J. Biol. Macromol.* 302 (2025) 139177, <https://doi.org/10.1016/j.ijbiomac.2024.139177>.
- [15] P. Mehta, A. Pawar, K. Mahadik, C. Bothiraja, Emerging novel drug delivery strategies for bioactive flavonol fisetin in biomedicine, *Biomed. Pharmacother.* 106 (2018) 1282–1291, <https://doi.org/10.1016/j.biopha.2018.07.079>.
- [16] S.-Y. Wang, L. Li, Y. Xiao, Y. Wang, Recent advances in cyclodextrins-based chiral-recognizing platforms, *TrAC Trends Anal. Chem.* 121 (2019) 115691, <https://doi.org/10.1016/j.trac.2019.115691>.
- [17] F. Bahavarnia, M. Hasanzadeh, P. Bahavarnia, N. Shadjou, Advancements in application of chitosan and cyclodextrins in biomedicine and pharmaceuticals: recent progress and future trends, *RSC Adv.* 14 (2024) 13384–13412, <https://doi.org/10.1039/D4RA01370K>.
- [18] G. Decool, M. Kfoury, L. Paitel, A. Sardo, S. Fourmentin, Cyclodextrins as molecular carriers for biopesticides: a review, *Environ. Chem. Lett.* 22 (2024) 321–353, <https://doi.org/10.1007/s10311-023-01658-3>.
- [19] Y. Miyah, N. El Messaoudi, M. Benjelloun, J. Georjin, D.S.P. Franco, M. El-habacha, O.A. Ali, Y. Acikbas, A comprehensive review of  $\beta$ -cyclodextrin polymer nanocomposites exploration for heavy metal removal from wastewater, *Carbohydr. Polym.* 350 (2025) 122981, <https://doi.org/10.1016/j.carbpol.2024.122981>.
- [20] S. Farooq, L. Xu, A. Ostovan, C. Qin, Y. Liu, Y. Pan, J. Ping, Y. Ying, Assessing the greenification potential of cyclodextrin-based molecularly imprinted polymers for pesticides detection, *Food Chem.* 429 (2023) 136822, <https://doi.org/10.1016/j.foodchem.2023.136822>.
- [21] N. Goyal, A. Amar, S. Gulati, R.S. Varma, Cyclodextrin-based Nanosponges as an environmentally sustainable solution for water treatment: A review, *ACS Appl. Nano Mater.* 6 (2023) 13766–13791, <https://doi.org/10.1021/acsanm.3c02026>.

- [22] M.J. Jozwiakowski, K.A. Connors, Aqueous solubility behavior of three cyclodextrins, *Carbohydr. Res.* 143 (1985) 51–59, [https://doi.org/10.1016/S0008-6215\(00\)90694-3](https://doi.org/10.1016/S0008-6215(00)90694-3).
- [23] E. Sabadini, T. Cosgrove, F.D.C. Egidio, Solubility of cyclomaltooligosaccharides (cyclodextrins) in H<sub>2</sub>O and D<sub>2</sub>O: A comparative study, *Carbohydr. Res.* 341 (2006) 270–274, <https://doi.org/10.1016/j.carres.2005.11.004>.
- [24] M. Kfoury, D. Landy, S. Fourmentin, Characterization of cyclodextrin/volatile inclusion complexes: A review, *Molecules* 23 (2018) 1204, <https://doi.org/10.3390/molecules23051204>.
- [25] W. Cai, T. Sun, X. Shao, C. Chipot, Can the anomalous aqueous solubility of  $\beta$ -cyclodextrin be explained by its hydration free energy alone? *Phys. Chem. Chem. Phys.* 10 (2008) 3236–3243, <https://doi.org/10.1039/b717509d>.
- [26] K.J. Naidoo, J.Y.J. Chen, J.L.M. Jansson, G. Widmalm, A. Maliniak, Molecular properties related to the anomalous solubility of  $\beta$ -Cyclodextrin, *J. Phys. Chem. B* 108 (2004) 4236–4238, <https://doi.org/10.1021/jp037704q>.
- [27] M. Bonini, S. Rossi, G. Karlsson, M. Almgren, P. Lo Nostro, P. Baglioni, Self-assembly of  $\beta$ -cyclodextrin in water. Part I: Cryo-TEM and dynamic and static light scattering, *Langmuir* 22 (2006) 1478–1484, <https://doi.org/10.1021/la052878f>.
- [28] T. Loftsson, P. Saokham, A.R. Sá Couto, Self-association of cyclodextrins and cyclodextrin complexes in aqueous solutions, *Int. J. Pharm.* 560 (2019) 228–234, <https://doi.org/10.1016/j.ijpharm.2019.02.004>.
- [29] A.R. Sá Couto, A. Ryzhakov, T. Loftsson, Self-assembly of  $\alpha$ -Cyclodextrin and  $\beta$ -Cyclodextrin: identification and development of analytical techniques, *J. Pharm. Sci.* 107 (2018) 2208–2215, <https://doi.org/10.1016/j.xphs.2018.03.028>.
- [30] A. Ryzhakov, T. Do Thi, J. Stappaerts, L. Bertoletti, K. Kimpe, A.R. Sá Couto, P. Saokham, G. Van den Mooter, P. Augustijns, G.W. Somsen, S. Kurkov, S. Inghelbrecht, A. Arien, M.I. Jimidar, K. Schrijnemakers, T. Loftsson, Self-assembly of Cyclodextrins and their complexes in aqueous solutions, *J. Pharm. Sci.* 105 (2016) 2556–2569, <https://doi.org/10.1016/j.xphs.2016.01.019>.
- [31] M. Kfoury, S. Fourmentin, State of the art in cyclodextrin solubility enhancement. Are green solvents the solution? *J. Mol. Liq.* 410 (2024) 125599, <https://doi.org/10.1016/j.molliq.2024.125599>.
- [32] W. Kunz, K. Holmberg, T. Zemb, Hydrotropes, *Curr. Opin. Colloid Interface Sci.* 22 (2016) 99–107, <https://doi.org/10.1016/j.cocis.2016.03.005>.
- [33] D.Y. Pharr, Z.S. Fu, T.K. Smith, W.L. Hinze, Solubilization of cyclodextrins for analytical applications, *Anal. Chem.* 61 (1989) 275–279, <https://doi.org/10.1021/ac00178a018>.
- [34] I. Shumilin, D. Harries, Cyclodextrin solubilization in hydrated reline: resolving the unique stabilization mechanism in a deep eutectic solvent, *J. Chem. Phys.* 154 (2021) 224505, <https://doi.org/10.1063/5.0052537>.
- [35] I. Shumilin, D. Harries, Enhanced solubilization in multi-component mixtures: mechanism of synergistic amplification of cyclodextrin solubility by urea and inorganic salts, *J. Mol. Liq.* 380 (2023) 121760, <https://doi.org/10.1016/j.molliq.2023.121760>.
- [36] M.A.R. Martins, S.P. Pinho, J.A.P. Coutinho, Insights into the nature of eutectic and deep eutectic mixtures, *J. Solut. Chem.* 48 (2019) 962–982, <https://doi.org/10.1007/s10953-018-0793-1>.
- [37] A.P. Abbott, G. Capper, D.L. Davies, R.K. Rasheed, V. Tambyrajah, Novel solvent properties of choline chloride/urea mixtures, *Chem. Commun.* (2003) 70–71, <https://doi.org/10.1039/b210714g>.
- [38] J.A. McCune, S. Kunz, M. Olesińska, O.A. Scherman, DESolution of CD and CB macrocycles, *Chem. Eur. J.* 23 (2017) 8601–8604, <https://doi.org/10.1002/chem.201701275>.
- [39] A. Triolo, F. Lo Celso, O. Russina, Structural features of  $\beta$ -Cyclodextrin solvation in the deep eutectic solvent, reline, *J. Phys. Chem. B* 124 (2020) 2652–2660, <https://doi.org/10.1021/acs.jpcc.0c00876>.
- [40] I. Shumilin, A. Tanbuz, D. Harries, Deep eutectic solvents for efficient drug solvation: optimizing composition and ratio for solubility of  $\beta$ -Cyclodextrin, *Pharmaceutics* 15 (2023) 1462, <https://doi.org/10.3390/pharmaceutics15051462>.
- [41] A. Triolo, F. Lo Celso, M. Brehm, V. Di Lisio, O. Russina, Liquid structure of a choline chloride-water natural deep eutectic solvent: A molecular dynamics characterization, *J. Mol. Liq.* 331 (2021) 115750, <https://doi.org/10.1016/J.MOLLIQ.2021.115750>.
- [42] A. Triolo, F. Lo Celso, S. Fourmentin, O. Russina, Liquid structure scenario of the archetypal supramolecular deep eutectic solvent: Heptakis(2,6-di-O-methyl)- $\beta$ -cyclodextrin/levulinic acid, *ACS Sustain. Chem. Eng.* 11 (2023) 9103–9110, <https://doi.org/10.1021/acssuschemeng.3c01858>.
- [43] E. Mangiacapre, A. Triolo, M. Kfoury, S. Ruellan, F. Lo Celso, D.J.M. Irving, S. Fourmentin, O. Russina, Sustainable aroma absorption: exploring the potentiality of a  $\beta$ -cyclodextrin and lactic acid supramolecular eutectic solvent, *Carbohydr. Polym.* 366 (2025) 123819, <https://doi.org/10.1016/j.carbpol.2025.123819>.
- [44] A. Triolo, F. Lo Celso, J. Perez, O. Russina, Solubility and solvation features of native cyclodextrins in 1-ethyl-3-methylimidazolium acetate, *Carbohydr. Polym.* 291 (2022) 119622, <https://doi.org/10.1016/j.carbpol.2022.119622>.
- [45] J.K. Percus, G.J. Yevick, Analysis of Classical Statistical Mechanics by Means of Collective Coordinates 110, 1958, <https://doi.org/10.1103/PhysRev.110.1>.
- [46] M. Kotlarchyk, S.H. Chen, Analysis of small angle neutron scattering spectra from polydisperse interacting colloids, *J. Chem. Phys.* 79 (1983) 2461–2469, <https://doi.org/10.1063/1.446055>.
- [47] B. Hess, C. Kutzner, D. van der Spoel, E. Lindahl, GROMACS 4: algorithms for highly efficient, load-balanced, and scalable molecular simulation, *J. Chem. Theory Comput.* 4 (2008) 435–447, <https://doi.org/10.1021/ct700301q>.
- [48] D. Van Der Spoel, E. Lindahl, B. Hess, G. Groenhof, A.E. Mark, H.J.C. Berendsen, GROMACS: fast, flexible, and free, *J. Comput. Chem.* 26 (2005) 1701–1718, <https://doi.org/10.1002/jcc.20291>.
- [49] C. Cézard, X. Trivelli, F. Aubry, F. Djedaini-Pilard, F.-Y. Dupradeau, Molecular dynamics studies of native and substituted cyclodextrins in different media: 1. Charge derivation and force field performances, *Phys. Chem. Chem. Phys.* 13 (2011) 15103–15121, <https://doi.org/10.1039/C1CP20854C>.
- [50] H. Zhang, C. Ge, D. Van Der Spoel, W. Feng, T. Tan, Insight into the structural deformations of beta-cyclodextrin caused by alcohol cosolvents and guest molecules, *J. Phys. Chem. B* 116 (2012) 3880–3889, <https://doi.org/10.1021/jp300674d>.
- [51] J. Gebhardt, C. Kleist, S. Jakobtorweihen, N. Hansen, Validation and comparison of force fields for native Cyclodextrins in aqueous solution, *J. Phys. Chem. B* 122 (2018) 1608–1626, <https://doi.org/10.1021/acs.jpcc.7b11808>.
- [52] B. Doherty, O. Acevedo, OPLS force field for choline chloride-based deep eutectic solvents, *J. Phys. Chem. B* 122 (2018) 9982–9993, <https://doi.org/10.1021/acs.jpcc.8b06647>.
- [53] W.L. Jorgensen, J. Chandrasekhar, J.D. Madura, R.W. Impey, M.L. Klein, Comparison of simple potential functions for simulating liquid water, *J. Chem. Phys.* 79 (1983) 926–935, <https://doi.org/10.1063/1.445869>.
- [54] L. Martínez, R. Andrade, E.G. Birgin, J.M. Martínez, PACKMOL: A package for building initial configurations for molecular dynamics simulations, *J. Comput. Chem.* 30 (2009) 2157–2164, <https://doi.org/10.1002/jcc.21224>.
- [55] G. Bussi, D. Donadio, M. Parrinello, Canonical sampling through velocity rescaling, *J. Chem. Phys.* 126 (2007) 014101, <https://doi.org/10.1063/1.2408420>.
- [56] M. Parrinello, A. Rahman, Polymorphic transitions in single crystals: A new molecular dynamics method, *J. Appl. Phys.* 52 (1981) 7182–7190, <https://doi.org/10.1063/1.328693>.
- [57] T. Darden, D. York, L. Pedersen, Particle mesh Ewald: an N-log(N) method for Ewald sums in large systems, *J. Chem. Phys.* 98 (1993) 10089–10092, <https://doi.org/10.1063/1.464397>.
- [58] U. Essmann, L. Perera, M.L. Berkowitz, T. Darden, H. Lee, L.G. Pedersen, A smooth particle mesh Ewald method, *J. Chem. Phys.* 103 (1995) 8577–8593, <https://doi.org/10.1063/1.470117>.
- [59] M. Brehm, M. Thomas, S. Gehrke, B. Kirchner, TRAVIS—A free analyzer for trajectories from molecular simulation, *J. Chem. Phys.* 152 (2020) 164105, <https://doi.org/10.1063/5.0005078>.
- [60] M. Brehm, B. Kirchner, TRAVIS - A free analyzer and visualizer for Monte Carlo and molecular dynamics trajectories, *J. Chem. Inf. Model.* 51 (2011) 2007–2023, <https://doi.org/10.1021/ci200217w>.
- [61] O. Hollóczki, M. Macchiagodena, H. Weber, M. Thomas, M. Brehm, A. Stark, O. Russina, A. Triolo, B. Kirchner, Triphasic ionic-liquid mixtures: fluorinated and non-fluorinated aprotic ionic-liquid mixtures, *ChemPhysChem* 16 (2015) 3325–3333, <https://doi.org/10.1002/cphc.201500473>.
- [62] O. Ferreira, L.P. Silva, H.H.S. Almeida, J. Benfica, D.O. Abbranches, S.P. Pinho, J.A.P. Coutinho, What is better to enhance the solubility of hydrophobic compounds in aqueous solutions: eutectic solvents or ionic liquids? *RSC Sustain.* 2 (2024) 4052–4060, <https://doi.org/10.1039/d4su00379a>.
- [63] G.A. Gaynanova, F.G. Valeeva, R.A. Kushnazarova, A.M. Bekmukhametova, S. V. Zakharov, A.B. Mirgorodskaya, L.Y. Zakharova, Effect of hydrotropic compounds on the self-organization and Solubilization properties of cationic surfactants, *Russ. J. Phys. Chem. A* 92 (2018) 1400–1405, <https://doi.org/10.1134/S0036024418070129>.
- [64] F.H.B. Sosa, D.O. Abbranches, A.M. da Costa Lopes, M.C. da Costa, J.A.P. Coutinho, Role of deep eutectic solvent precursors as Hydrotropes: unveiling synergism/antagonism for enhanced Kraft lignin dissolution, *ACS Sustain. Chem. Eng.* 12 (2024) 8930–8940, <https://doi.org/10.1021/acssuschemeng.4c02529>.
- [65] A.F.M. Cláudio, M.C. Neves, K. Shimizu, J.N. Canongia Lopes, M.G. Freire, J.A.P. Coutinho, The magic of aqueous solutions of ionic liquids: ionic liquids as a powerful class of cationic hydrotropes, *Green Chem.* 17 (2015) 3948–3963, <https://doi.org/10.1039/c5gc00712g>.
- [66] T.E. Sintra, D.O. Abbranches, J. Benfica, B.P. Soares, S.P.M. Ventura, J.A.P. Coutinho, Cholinium-based ionic liquids as bioinspired hydrotropes to tackle solubility challenges in drug formulation, *Eur. J. Pharm. Biopharm.* 164 (2021) 86–92, <https://doi.org/10.1016/j.ejpb.2021.04.013>.
- [67] J. Benfica, A.C. Martins, G. Pérez-Sánchez, N. Schaeffer, J.A.P. Coutinho, Exploring the impact of sodium salts on hydrotropic solubilization, *Phys. Chem. Chem. Phys.* 25 (2023) 26327–26340, <https://doi.org/10.1039/d3cp02034g>.
- [68] S. Jin, X. Cui, Y. Qi, Y. Shen, H. Li, Measurement and correlation of the solubility of  $\beta$ -Cyclodextrin in different solutions at different temperatures and thermodynamic study of the dissolution process, *Processes* 7 (2019), <https://doi.org/10.3390/pr7030135>.
- [69] O. Kuzmina, E. Bordes, J. Schmauck, P.A. Hunt, J.P. Hallett, T. Welton, Solubility of alkali metal halides in the ionic liquid [C4C1im][OTf], *Phys. Chem. Chem. Phys.* 18 (2016) 16161–16168, <https://doi.org/10.1039/c6cp02286c>.
- [70] M.T. Stone, P.J. Int Veld, Y. Lu, I.C. Sanchez, Hydrophobic/hydrophilic solvation: inferences from Monte Carlo simulations and experiments, *Mol. Phys.* 100 (2002) 2773–2792, <https://doi.org/10.1080/00268970210139912>.
- [71] B. Hribar, N.T. Southall, V. Vlachy, K.A. Dill, How ions affect the structure of water, *J. Am. Chem. Soc.* 124 (2002) 12302–12311, <https://doi.org/10.1021/ja026014h>.
- [72] Y. Zheng, X. Xuan, J. Wang, M. Fan, The enhanced dissolution of  $\beta$ -cyclodextrin in some hydrophilic ionic liquids, *J. Phys. Chem. A* 114 (2010) 3926–3931, <https://doi.org/10.1021/jp907333v>.
- [73] T. Moufawad, L. Moura, M. Ferreira, H. Bricout, S. Tilloy, E. Monflier, M. Costa Gomes, D. Landy, S. Fourmentin, First evidence of Cyclodextrin inclusion

- complexes in a deep eutectic solvent, ACS sustain. Chem. Eng. 7 (2019) 6345–6351, <https://doi.org/10.1021/acssuschemeng.9b00044>.
- [74] L. Szente, J. Jo, J. Szejtli, G.L. Kis, Spontaneous opalescence of aqueous  $\gamma$ -Cyclodextrin solutions: complex formation or self-aggregation? J. Pharm. Sci. 87 (1998) 778–781, <https://doi.org/10.1021/js9704341>.
- [75] A.W. Coleman, I. Nicolis, N. Keller, J.P. Dalbiez, Aggregation of Cyclodextrins: an explanation of the abnormal solubility of  $\gamma$ -Cyclodextrin, J. Incl. Phenom. Macrocycl. Chem. 13 (1992) 139–143, <https://doi.org/10.1007/BF01053637>.
- [76] K. Miyajima, M. Sawada, M. Nakagaki, Viscosity B-coefficients, apparent molar volumes, and activity coefficients for  $\alpha$ - and  $\gamma$ -Cyclodextrins in aqueous solutions, Bull. Chem. Soc. Jpn. 56 (1983) 3556–3560, <https://doi.org/10.1246/bcsj.56.3556>.
- [77] G. González-Gaitano, P. Rodríguez, R. Rodríguez, J.R. Isasi, M. Fuentes, G. Tardajos, M. Sánchez, The Aggregation of Cyclodextrins as Studied by Photon Correlation Spectroscopy, 2002, <https://doi.org/10.1023/A:1023065823358>.
- [78] A. Kusmin, R.E. Lechner, M. Kammel, W. Saenger, Native and methylated cyclodextrins with positive and negative solubility coefficients in water studied by SAXS and SANS, J. Phys. Chem. B 112 (2008) 12888–12898, <https://doi.org/10.1021/jp802031w>.
- [79] A.J.M. Valente, R.A. Carvalho, O. Söderman, Do Cyclodextrins aggregate in water? Insights from NMR experiments, Langmuir 31 (2015) 6314–6320, <https://doi.org/10.1021/acs.langmuir.5b01493>.
- [80] A.J.M. Valente, R.A. Carvalho, D. Murtinho, O. Söderman, Molecular dynamics of Cyclodextrins in water solutions from NMR deuterium relaxation: implications for Cyclodextrin aggregation, Langmuir 33 (2017) 8233–8238, <https://doi.org/10.1021/acs.langmuir.7b01923>.
- [81] P. Saokham, C. Muankaew, P. Jansook, T. Loftsson, Solubility of cyclodextrins and drug/cyclodextrin complexes, Molecules 23 (2018), <https://doi.org/10.3390/molecules23051161>.
- [82] P. Jansook, M.D. Moya-Ortega, T. Loftsson, Effect of self-aggregation of  $\gamma$ -cyclodextrin on drug solubilization, J. Incl. Phenom. Macrocycl. Chem. 68 (2010) 229–236, <https://doi.org/10.1007/s10847-010-9779-3>.
- [83] G. Raffaini, F. Ganazzoli, Hydration and flexibility of  $\alpha$ -,  $\beta$ -,  $\gamma$ - and  $\delta$ -cyclodextrin: A molecular dynamics study, Chem. Phys. 333 (2007) 128–134, <https://doi.org/10.1016/j.chemphys.2007.01.015>.